SUPPLEMENTAL INFORMATION

High-Throughput Dental Biofilm Growth Analysis for Multiparametric Microenvironmental Biochemical Conditions Using Microfluidics

Raymond H. W. Lam,*[abc], Xin Cui[a], Weijin Guo[a], and Todd Thorsen*[d]

[a] Department of Mechanical and Biomedical Engineering, City University of Hong Kong, Hong Kong
[b] Centre for Robotics and Automation, City University of Hong Kong
[c] Centre for Biosystems, Neuroscience and Nanotechnology, City University of Hong Kong
[d] Department of Mechanical Engineering, Massachusetts Institute of Technology, Boston, USA

*Correspondence should be addressed to both RHW Lam (email address: rhwlam@cityu.edu.hk; Tel: +852-3442-8577, Fax: +852-3442-0172) and T Thorsen (email address: thorsen@mit.edu).

S1 Detailed Fabrication Process

Multiple negative molds for replica molding using soft lithography were first prepared: 1) Molds for the gas control layer, the upper flow control layer and the water jacket were fabricated using photolithography of SU-8 2010 (Microchem) with the same thickness of 20 μm on 3" silicon wafers. 2) A mold for the lower flow control layer, which contained also the micro-mixers, included two SU-8 layers with 100 μm tall via-hole structures (SU-8 2050, Microchem) located on top of the 20 μm thick water jacket microstructures. 3) Another mold for the chamber layer included a layer of SU-8 2100 (Microchem) with a thickness of 200 μm on a wafer was also fabricated. 4) A mold for the gas layer and the inlet channels for water jackets was fabricated with a two-step photolithography process, which involved firstly patterning the lower 10 μm thick layer (SU-8 2010), followed by adhesion promotion with hexamethyldisilazane (Sigma-Aldrich, St. Louis, MO) and patterning of AZ4620 photoresist (AZ Electronic Materials) with a thickness of 20 μm for the valve-controllable regions. 5) A mold for the flow layer was fabricated by photolithography of AZ4620 photoresist (thickness: 20 μm) with adhesion promotion of hexamethyldisilazane. After the photolithography process, all the molds were baked on a 90 °C hotplate for 2 min to further cross-link the SU-8 layers. The molds for the gas and flow layers were then baked on a hotplate at 140 °C on a hotplate for 1 min to reflow the AZ4620 microstructures. Finally, all the molds were silanized with a high-molecular-weight trichloro-perfluorooctyl silane (Sigma-Aldrich) to facilitate the PDMS peeling-off from the molds in the later processes.

We applied multilayer soft lithography to fabricate the artificial teeth chip as described in **Fig. S1**. The structural material was prepared by mixing PDMS monomer and curing agent

(Sylgard 184, Dow Corning, Midland, Michigan) with a 10:1 weight ratio. The PDMS pre-polymer was poured on the mold for gas control layer with a thickness of ~5 mm contained in a petri dish, followed by baking it for 25 min in an oven at 80 °C (***Step 1***). Other structural PDMS layers were prepared by spin-coating the pre-polymer on the molds with different thickness: 40 μm for the gas layer, 80 μm for the water jacket, 220 μm for the upper flow control layer and 40 μm for the flow layer. The PDMS pre-polymer on the gas mold was baked at 80 °C for 15 min for the partial-crosslinking; whereas other PDMS pre-polymer layers were baked at 80 °C with their molds for 2 hr until fully cured (***Step 2***). The PDMS gas control layer was cut with a razor blade (Cat# 55411-050, VWR, Radnor, PA) and peeled off from the mold with its gas inlets by punching (Cat# 09923355, Thermo Fisher Scientific, Grand Island, NY). The peeled-off PDMS substrate was aligned on the partially cured PDMS gas layer under a stereomicroscope and further baked at 80 °C for 2 hr. After cutting, peeling off and punching holes on the PDMS substrate with the gas control and gas layers (***Step 3***), the gas channel side of this substrate and the PDMS water jacket layer were treated with oxygen plasma (Plasmod, Tegal Corporation, 600 mTorr) at 50 W RF power for 15 s. The PDMS substrate was then aligned on the water jacket layer under a stereomicroscope, before baking the stacked substrate for an additional 2 hr. After cutting device edges, peeling off the substrate and punching for the gas inlets/outlets, the via-holes along gas inlet channels between the gas flow layer and the water jacket layer were generated by cutting away the holes with a razor blade (***Step 4***). Again, the PDMS substrate (the water jacket side) and the upper flow control layer were then plasma-treated, aligned together under a stereomicroscope, and baked at 80 °C for another 2 hr. The PDMS substrate was cut, peeled-off and punched for inlets/outlets (***Step 5***).

On the other hand, the lower flow control layer was prepared separately. We poured the PDMS pre-polymer onto the lower flow control mold and cover the PDMS with a polyester film. We sandwiched the mold consisting of the PDMS and an overhead polyester film between two acrylic sheets (thickness: 5 mm). We then applied compressive pressure on the PDMS layer by clamping the acrylic sheets such that the PDMS pre-polymer on via-hole microstructures of the mold was squeezed aside, followed by baking the entire clamped specimen at 80 °C for 2 hr (***Step 6***). We finished fabrication of the lower flow control layer by removing the clamps, the acrylic sheets and the polyester film. This PDMS structure consisting of the gas control channels down to the upper flow control channels and the previously prepared lower flow control layer were treated by oxygen plasma and aligned together under a stereomicroscope. After baking at 80 °C for 2 hr, the PDMS substrate was

cut, peeled-off and punched at the control inlets accordingly (***Step 7***). Next, the PDMS substrate and the flow layer were then plasma-treated, aligned together under a stereomicroscope, and baked at 80 °C for another 2 hr. The combined PDMS substrate was cut, peeled-off and punched for inlets/outlets (***Step 8***).

We prepared the chamber layer by pouring the PDMS pre-polymer onto the chamber mold with a thickness of ~800 μm (***Step 9***). We baked the sample for thorough cross-linking, cut the edges, peeled off the PDMS chamber layer and bonded this layer on a glass slide (Cat # 16004-422, VWR) by oxygen plasma with the microwell-structure side facing outside. We then deposited polystyrene layers into all the microwells by applying 0.3 nL of 5 % (w/w) dissolved polystyrene in toluene. The polystyrene layers would form after the toluene evaporated (***Step 10***). Finally, we finished the device fabrication process by bonding the multilayer PDMS substrate with the microwell-array substrate using oxygen plasma (***Step 11***).

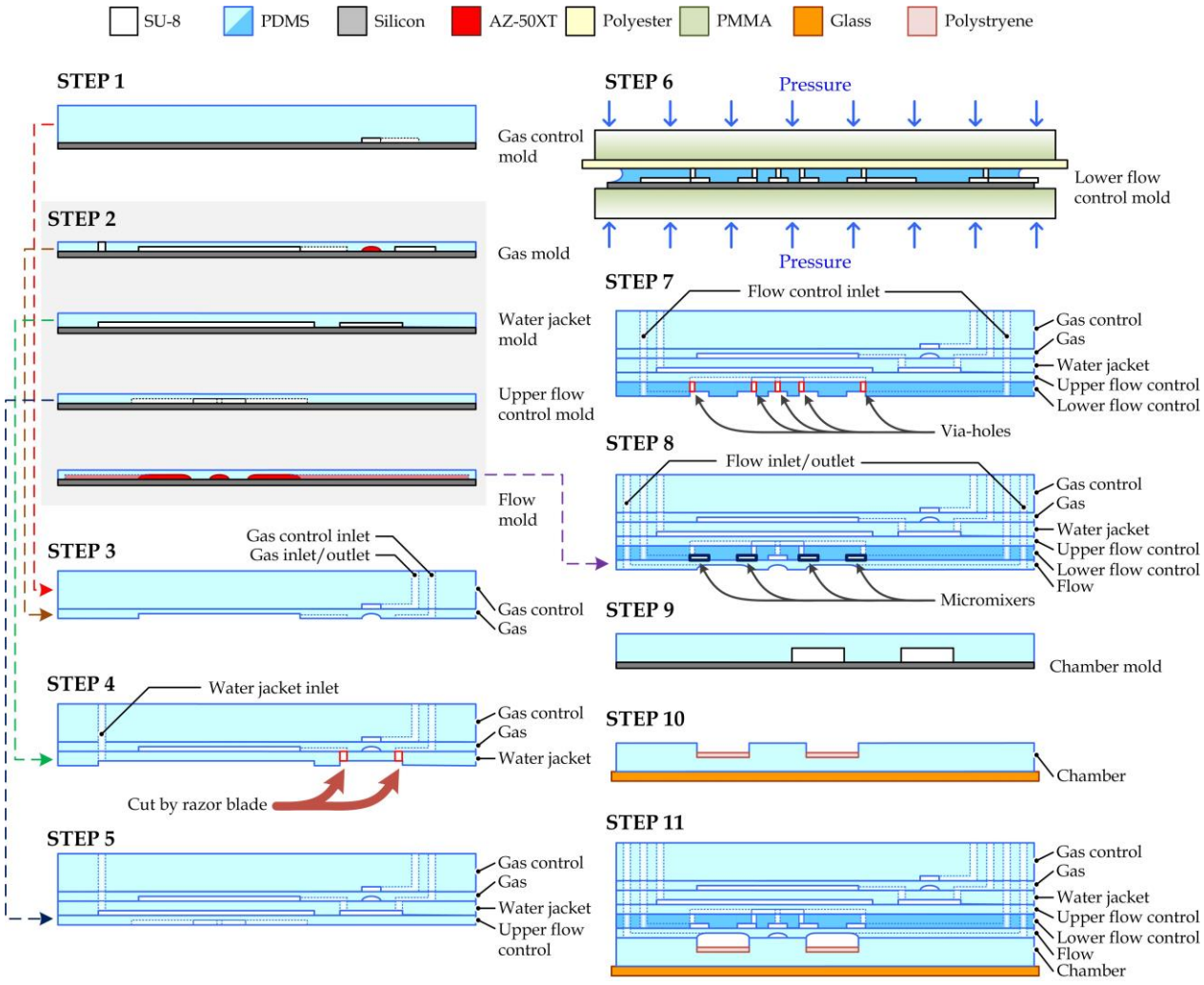

Figure S1. Fabrication process of the microfluidic artificial teeth device. Geometry and dimensions are different from the actual device and are shown here for describing the key features only.

S2 Substrate Material Selection and Surface Treatment

Microbial adhesion is a prerequisite to initiate dental biofilm formation; therefore the substrate material should support the initial attachment of primary colonizers as the foundation for subsequent biofilm development in the artificial teeth device. It has been reported that the salivary pellicle-coated film can be formed on various materials (glass[1], plastic and hydroxyapatite[2]) to regulate the surface conditions (*e.g.* biochemical compositions, ion supply, surface energy, zeta potential and hydrophobicity[3]) of human teeth and facilitate the adhesion of dental bacteria to their specific receptors[4]. For instance, specific components, such as salivary glycoprotein, can serve as receptors for oral *Streptococci* in the salivary pellicle[5].

We prepared *Streptococcus sanguinis*, which is one of the major early colonizers in dental biofilm, for further examining the bacterial attachment on different saliva-coated substrate materials. *S. sanguinis* were pre-cultured in brain heart infusion broth (Hardy Diagnostics R20). Culturing was performed in an incubator with a rotary shaking platform (200 rpm) at 37 ºC for 20 hr. Because microbial clusters can be found in the culture, causing inconsistent cell densities during cell loading. The bulk culture was first re-suspended by pipetting (>50 times) to scatter the aggregated cells into smaller communities. The cells were then cultured at 37 ºC for 30 min without shaking to allow sedimentation of the cell clusters. Samples extracted from the top portion of culture were seeded on the substrate material candidates (glass, PDMS and polystyrene).

We conducted experiments to investigate the attachment of *Streptococci* (*S. sanguinis*) on three candidate materials (glass, polystyrene and PDMS) with the filtered-saliva coating. We would like to select the material with the better bacterial attachment for biofilm culture experiments using the artificial teeth device as mentioned in the main-text. We prepared 1) the glass substrate with a coverslip, 2) a spin-coated PDMS film (thickness: 10 μm) fully cured on glass, and 3) a polystyrene film (thickness: < 5 μm) deposited on a coverslip. Fabrication of the polystyrene layer started with dissolving polystyrene in toluene solution with a weight ratio of 5 %, followed by pipetting the solution on a coverslip (~200 nL per cm^2). The polystyrene film was then formed after toluene evaporated. For the surface conditioning, human saliva filtered by the filtration bottle (Cat# 8-0000-42 0803, Nalgene Labware, Inc.) was applied on the different substrates for > 1 hr. The substrates were then placed in basal media mucin with the *Streptococci* at a density of ~10^7 cells/mL and incubated for 15 min. After rinsing gently with phosphate-buffered saline (PBS), phase contrast microscopic images were taken as shown in **Fig. S2a**. Results show that the

Streptococci had better adherence on polystyrene than glass and PDMS. Furthermore, we performed the adherence test of the *Streptococci* on polystyrene with different incubation durations. Results (**Fig. S2b** and **S2c**) indicate that the number of attached cells increased with the incubation time (1 – 10 min) and became saturated with cell coverage of ~3.2×10^6 cells/cm^2 for ≥ 10 min incubation. Hence, to ensure achieve better attachments of *Streptococci* and other early colonizers, we selected polystyrene as the substrate material and we applied a primary incubation of filtered saliva in every culture chamber prior to insertion of bacteria samples in the dental biofilm culture experiments using the artificial teeth devices.

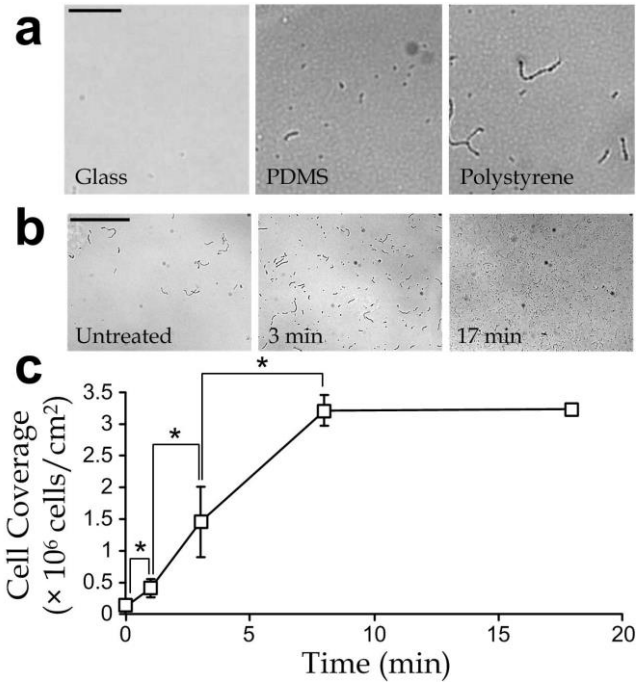

Figure S2. (**a**) Attachment of *Streptococci* on different substrate materials: polystyrene, glass and PDMS conditioned with filtered human saliva. Scale bar: 50 μm. (**b**) Micrographs (scale bar: 200 μm) and (**c**) cell coverage of attached *Streptococci* to the surface-conditioned polystyrene substrate as a function of incubation time (N = 8).

S3 Capture and Deconvolution of Fluorescence Image Stacks

As mentioned in the main-text, the artificial teeth device was placed on the motorized stage of our previously developed automated microscope system throughout biofilm culture. After the biofilm culture and cell staining procedures, a stack of microscopic fluorescence images was taken by the automated microscope system at every chamber, from 40 μm below the polystyrene substrate to 40 μm above the chamber celling with a separating distance between images of 2 μm. Movements of the microscope stage along z-direction was controlled by the automated microscope system[32]. Notably, these images appeared to be burry, mainly caused by optical distortions of fluorescence

emission from the staining probes such as axial smearing and spherical aberrations[6]. In other words, the intensity value shown by a pixel in a captured image was the total overlapped intensity of all optical distortions around the pixel region in all *x*, *y* and *z*-directions[7].

In principle, optical transformation from the raw stained biofilm body to the 'blurred' three-dimensional intensity profile can be considered as the convolution of the raw biofilm body and a point-spread function (PSF), which is the impulse response representing the resultant optical profile of a fluorescent pixel volume. PSF can be estimated with key parameters including the refractive index of culture media, numerical aperture, wavelength of the emission light, distance between two consecutive image slices, and length represented by a pixel width. Hence, we may apply deconvolution using the captured image stacks and PSF to compute geometry of the stained biofilm body. In this work, we have adopted the image deconvolution algorithm provided by commercial software (Huygens Deconvolution Software, Scientific Volume Imaging) in order to suppress the intensity dispersion caused by reemission of the fluorescence stains. As demonstration, an image slice of the stained live cells in a biofilm shown in **Fig. S3a** indicates an effective removal of the intensity dispersion. **Fig. S3b** shows the image slices of the biofilm **Fig. 4a** at different z-positions.

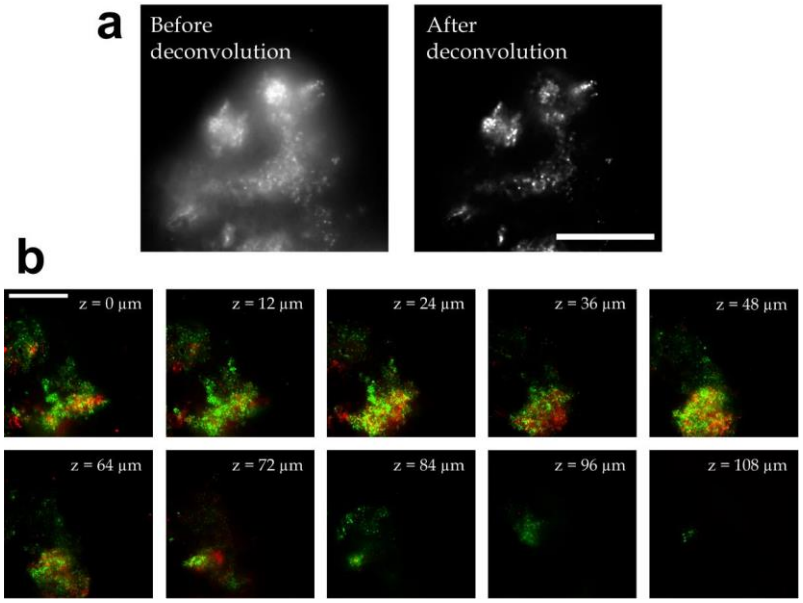

Figure S3. (**a**) Sample image slice of live cells in a biofilm before (*left*) and after (*right*) the image deconvolution process. Scale bar: 100 µm. (**b**) Sample deconvoluted image slices of live (*green*) and dead (*red*) cells at different vertical (*z*) levels in a dental biofilm, cultured in an artificial teeth device. Scale bar: 100 µm.

S4 Image Processing for Population Ratio of Live-Dead Bacteria as a Function of Depth from Biofilm Surface.

As mentioned in the main-text, we applied three-dimensional image process techniques to classify biofilm volumes into layers in terms of different ranges of the depth from the biofilm surface. Technically, we first performed intensity thresholding to identify the whether a pixel in an image stack was part of the biofilm (*i.e.* '1' represents the biofilm body, and '0' represents the background).

We then iteratively applied the three-dimensional binary erosion operation on the processing image stack. Considering the pixel width in each image slice corresponded to a physical width of 0.5 μm and the distance between consecutive image slices was 2 μm, we have designed an 'erosion' mask to remove 4 pixels in both positive/negative *x*-direction and positive/negative *y*-direction, and 1 pixel in positive/negative *z*-direction. It should be mentioned that the lower biofilm-pixels attaching to the chamber base would not be removed by this erosion operation.

We classified the biofilm as multiple layers, with each had a thickness of ~4 μm. Hence, we removed each ~4 μm thick biofilm layer by two erosion operations. We considered the pixels removed by such erosion process as a biofilm layer. By iteratively performing the biofilm surface extraction process with the two-time erosion, we could classify the biofilm body as multiple layers with different depths from the outmost biofilm surface. We then calculated the live-dead cell ratios within each of the biofilm layers.

S5 Oligonucleotide Probes Adopted for FISH Identification

Table S1. Oligonucleotide probes for identification of species with different sequences and the corresponding 5'-modifications

Probe	Target	5'-3' Sequence	5'-modification ($\lambda_{excitation}$, $\lambda_{emission}$) [nm]	Ref.
STR 405	*Streptococcus spp.*	TAGCCGTCCCTTTCTGGT	Fluorescein (494, 521)	8
FUS664	*F. nucleatum*	CTTGTAGTTCGC(C/T)TACCTC	Texas Red (589, 615)	8
IF 201	*A. naeslundii*	GCTACCGTCAACCCACCC	Cy 5.5 (675, 694)	8
POGI	*P. gingivalis*	CAATACTCGTATCGCCCGTTATTC	IRD 800 (780, 816)	9

References

1. H. Mukasa and H. D. Slade, Infection and Immunity, 1974, 9, 419-429.
2. R. Gibbons, E. Moreno and I. Etherden, Infection and Immunity, 1983, 39, 280-289.

3. W. Teughels, N. Van Assche, I. Sliepen and M. Quirynen, Clinical oral Implants Research, 2006, 17, 68-81.
4. J. D. Rudney, R. Chen, P. Lenton, J. Li, Y. Li, R. S. Jones, C. Reilly, A. S. Fok and C. Aparicio, Journal of Applied Microbiology, 2012, 113, 1540-1553.
5. A. Hodgson, S. Nelson, M. Brown and P. Gilbert, Journal of Applied Bacteriology, 1995, 79, 87-93.
6. P. Pankajakshan, B. Zhang, L. Blanc-Féraud, Z. Kam, J.-C. Olivo-Marin and J. Zerubia, Applied optics, 2009, 48, 4437-4448.
7. T. Saggese, A. A. Young, C. Huang, K. Braeckmans and S. R. McGlashan, *Cilia*, 2012, **1**, 1.
8. A. Al-Ahmad, A. Wunder, T. M. Auschill, M. Follo, G. Braun, E. Hellwig and N. B. Arweiler, Journal of medical microbiology, 2007, 56, 681-687.
9. F. Cavrini, V. Sambri, A. Moter, D. Servidio, A. Marangoni, L. Montebugnoli, F. Foschi, C. Prati, R. Di Bartolomeo and R. Cevenini, Journal of Medical Microbiology, 2005, 54, 93-96.